

Specific Emitter Identification Based on RepVGG and Gramian Angular Field

Deguo Zeng¹, Fuyuan Xu¹✉, Jin Qin¹, Zhenyi Yao², Zuyue Shang¹

(1. Nanjing Electronic Equipment Institute, Nanjing 210016, China; 2. College of Automation, Nanjing University of Aeronautics and Astronautics, Nanjing 211106, China)

Abstract: This paper presents a new method for specific emitter identification (SEI) using the re-parameterization visual geometry group (RepVGG) neural network model and Gramian angular summation field (GASF). It converts in-phase and quadrature (IQ) signals into 2D feature maps, retaining both time and frequency domain features. Compared to residual network 18-layer (ResNet18) and Hilbert transform methods, this approach offers higher accuracy, faster training, and a smaller model size, making it ideal for hardware deployment.

Keywords: specific emitter identification; re-parameterization visual geometry group (RepVGG); Gramian angular field

1 Introduction

Specific emitter identification (SEI) is a crucial component of radar, reconnaissance, and early warning systems, as it provides the military with precise intelligence regarding adversary radar installations. Through the analysis of intercepted electromagnetic signals, SEI seeks to distinctly identify individual radar radiation sources in situations where all platforms and presumed intercepted signal parameters are analogous, thereby offering essential intelligence for electronic protection systems in military operations.

In the initial specific emitter identification tasks, methodologies reliant on traditional features, such as pulse descriptors and pulse repetition interval (PRI), are typically employed. Nevertheless, advancements in technology have rendered traditional individual recognition methods inadequate for the contemporary intricate elec-

tromagnetic environment, resulting in the emergence of many novel feature computation techniques. The most recent types of features can be broadly classified as time-domain features, frequency-domain features, and time-frequency-domain features. Concurrently, machine learning and deep learning algorithms have progressively emerged as standard instruments for enhancing categorization precision.

In Ref. [1], following the enhancement of the signal-to-noise ratio through precise time alignment and coherent integration of the received radar pulses, variable mode decomposition (VMD) is employed to deconstruct the envelope and instantaneous frequency of the received signals into a collection of characteristics. The findings indicate that the strategy enhances the signal-to-noise ratio and the precision of individual identification. A structure called multi-scale attention kernel (MSAK) combined with convolutional neural network (CNN) and long short-term memory (LSTM) networks is proposed in Ref. [2]. The proposed model demonstrates satisfactory accuracy in identifying unknown emitters in open environments and exhibits advan-

Manuscript received Mar. 7, 2025; revised Sep. 18, 2025; accepted Oct. 19, 2025. The associate editor coordinating the review of this manuscript was Dr. Junjie Wu. This work was supported by the National Natural Science Foundation of China (No. 62027801).

✉ Corresponding author. Email: xufuyuan818@gmail.com
DOI: [10.15918/j.jbit1004-0579.2025.015](https://doi.org/10.15918/j.jbit1004-0579.2025.015)

tages in linear-to-noise ratio (SNR) conditions. Refs. [3–6] have employed the envelope information of radar emissions to extract characteristics. Subsequently, the envelope characteristics were computed, including the rising edge, falling edge, top drop, pulse width, higher-order moments, and more features; ultimately, input these features into a classifier to facilitate identification. Ref. [7] developed a 1D-CNN model with two convolutional layers, one pooling layer, and two fully connected layers, utilizing spectral characteristics as input data for SEI. Ref. [8] developed a 1D-CNN model utilizing the attention mechanism with raw time series inputs, achieving commendable performance for SEI.

The previously stated SEI approaches utilizing deep learning used one-dimensional sequences or two-dimensional frequency-domain feature maps as input, neglecting the time-domain characteristics of the signal component. This study presents the construction of the re-parameterization visual geometry group (RepVGG) neural network model. The in-phase and quadrature (IQ) signal is converted into a two-dimensional feature map using the Gramian angular summation field (GASF) to retain both temporal and frequency domain characteristics. This method enhances the performance of the SEI.

2 Basic Theory

2.1 GASF

The GASF is a technique for transforming time series data into two-dimensional representations. The Gramian angular matrix is utilized to represent the dynamic features of the data in a static image format.

The Gramian angular matrix is a symmetric positive definite matrix derived from the inner product of time series data. Each matrix element denotes the cosine of the angle between the data points at the specified time point. Mapping the components of the Gramian angular matrix to the pixel values of the image results in the forma-

tion of a two-dimensional Gramian angle field. Given a time series $X = \{x_1, x_2, \dots, x_N\}$ of length N , the first step in constructing the GASF is to scale the data to the interval $[-1, 1]$ to ensure compatibility with cosine encoding. This is achieved via min-max scaling followed by a linear transformation[9]:

$$\tilde{x}_i = \frac{(x_i - \max(X)) + (x_i - \min(X))}{\max(X) - \min(X)} \quad (1)$$

where x_i represent the i th data point of the original time series, \tilde{x}_i denoted the scaled data point, $\max(X)$ and $\min(X)$ indicate the maximum and minimum values of the original time series X respectively. The time series is expressed in polar coordinates, with the value encoded as angular cosine and the timestamp represented as radius.

$$\begin{cases} \phi = \arccos(\tilde{x}_i), -1 \leq \tilde{x}_i \leq 1, \tilde{x}_i \in \tilde{X} \\ r = \frac{t_i}{N}, t_i \in \mathbb{N} \end{cases} \quad (2)$$

where ϕ indicates the polar angle, r indicates the polar diameter, t_i indicates the timestamp, and N indicates the total length of the time series.

The GASF representation emphasizes long-term dependencies and global structure in the time series, as each entry reflects a nonlinear combination of two time points. Moreover, because the transformation is deterministic and invertible (under certain conditions), it preserves essential characteristics of the original signal. This 2D representation can then be used directly as input to image-based models.

2.2 RepVGG

RepVGG employs an architecture similar to that of visual geometry group (VGG), characterized by its plain structure. The approach employs a multi-branch model during training and subsequently transforms this model into a single path model for inference. The convolution module is outlined as follows

$$y = x + g(x) + f(x)$$

where x , $g(x)$, $f(x)$ correspond to constant mapping, 1×1 convolution and 3×3 convolution

respectively. During training, parallel 1×1 convolutional branches and constant mapping branches are added to each 3×3 convolutional layer to form a RepVGG block. The multi-branch structure is then transformed into a 3×3 one-way convolution by structural reparameterization in inference mode. The reparameterization process is illustrated by Fig. 1 [10].

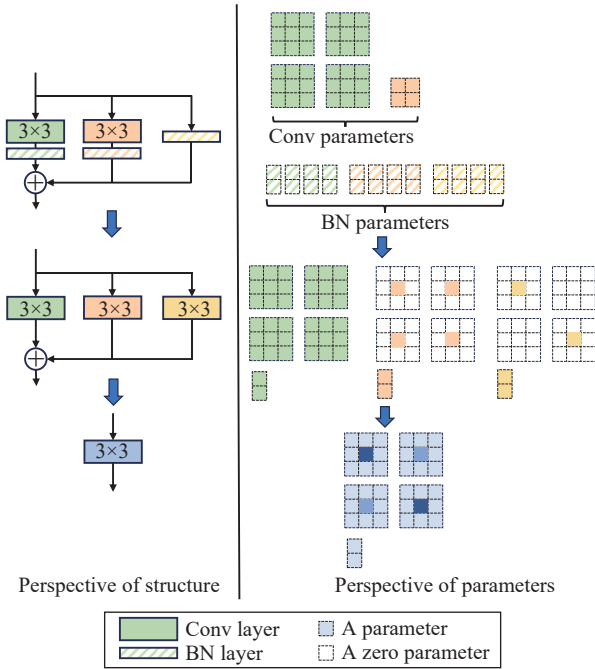


Fig. 1 Structural re-parameterization[7]

3 Specific Emitter Identification Based on RepVGG and Gramian Angular Field

GASF effectively maintains the temporal characteristics of the data while producing a consistent 2D feature map for a specific time series, thereby preventing the loss of feature information. The creation of 2D feature maps imparts spatial char-

acteristics to the data, thereby enhancing the recognition accuracy of the network. Furthermore, GASF produces 2D feature maps utilizing minimal data, resulting in reduced costs for data collection and storage, while also preventing sample overlap [11].

This paper utilizes quadrature IQ signals from a specific radar type. The IQ signals, referred to as isotropic quadrature signals, consist of I , which is in-phase, and Q , which is quadrature, exhibiting a phase difference of 90° from I . The IQ signal must first be modulated to create three channels: in-phase, quadrature, and modulus. Wherein the modulus M is

$$M = \sqrt{I^2 + Q^2} \tag{3}$$

Fig. 2 illustrates the conversion of three-channel data into three feature maps, each measuring 256×128 , through the use of GASF. It is then spliced into a tensor of dimensions $3 \times 256 \times 128$ along the channel direction.

The spliced tensor is input into the RepVGG convolutional layer, and the specific emitter identification process is illustrated in Fig. 3.

4 Experimental Results and Analysis

4.1 Gramian Angular Summation Field

This article presents signals from 10 radar targets, each comprising 3000 samples. This research presents a dataset of 30000 randomly disturbed pieces, divided into three categories: training set, validation set, and test set, with the following ratio among the categories: 7:2:1. Each target has 2100 pieces of data in the training set, 600 pieces of data in the validation set, and

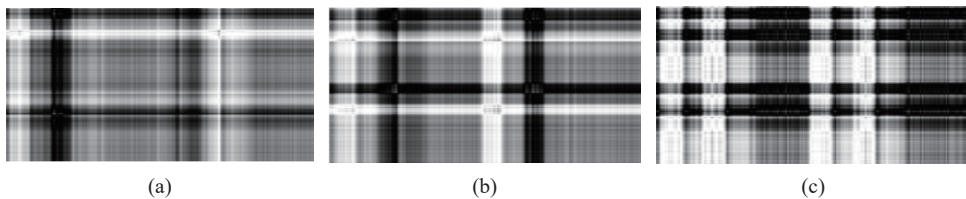


Fig. 2 2D feature maps of each channel after GASF: (a) in-phase; (b) quadrature; (c) model

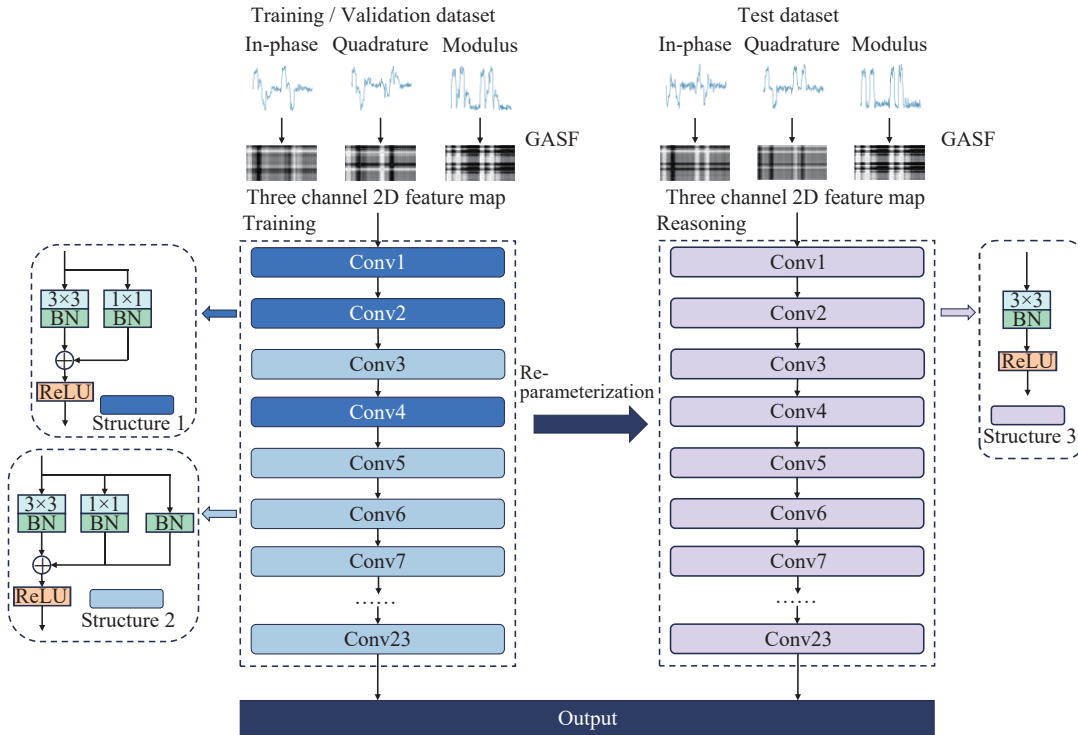


Fig. 3 Process of specific emitter identification

300 pieces of data in the test set. The particular components of the dataset are presented in Tab. 1.

Tab. 1 Component of dataset

Target	Training set	Validation set	Test set
Target1	2100	600	300
Target2	2100	600	300
Target3	2100	600	300
Target4	2100	600	300
Target5	2100	600	300
Target6	2100	600	300
Target7	2100	600	300
Target8	2100	600	300
Target9	2100	600	300
Target10	2100	600	300

4.2 Comparison Experiment

This research use residual network 18-layer (ResNet18) as the neural network model for comparison and utilizes the standard Hilbert transform for two-dimensional feature map extraction for comparison purposes. ResNet18 is a prominent neural network model, and its input dimensions align with those of RepVGG, rendering it suitable as a control group. This paper employs RepVGG-A0 and ResNet18 as neural

networks, while GASF and Hilbert transform serve as data enhancement techniques, resulting in four experimental groups formed by their pairwise combinations.

The identical training parameters and equipment were utilized on all four occasions. The particulars are as follows: The learning rate undergoes exponential decay, commencing at 0.001 with a decay rate of 0.95, the Adam optimizer is employed; the batch size is 32, and the total number of iterations is 30. The training process was expedited by the graphics processing unit (GPU), utilizing an computer with advanced micro devices (AMD) Ryzen 75800H, 16 GB of random access memory (RAM) and an NVIDIA RTX 3060.

During the model's training phase, an early stopping mechanism is employed to prevent overfitting. Specifically, a flag is activated to terminate training prematurely if the validation loss increases for three consecutive epochs. This threshold of three consecutive increases was selected based on a balance between sensitivity to overfitting and robustness to minor fluctua-

tions in validation loss. A smaller threshold (e.g., two) might halt training too early due to stochastic variations during training, while a larger threshold (e.g., four or five) could allow excessive overfitting before intervention. Upon triggering the stopping criterion, the model weights from the first of the three consecutive sessions are preserved as the final trained model. The experimental results are presented in Tab. 2.

Tab. 2 Experiment’s results

Method	Accuracy (%)	Training time (s)	Model size (MB)
RepVGG-A0 + GASF	98.08	3934	30.1
ResNet18 + GASF	98.07	4832	53.4
RepVGG-A0 + Hilbert	96.88	3945	30.1
ResNet18 + Hilbert	97.16	4481	53.4

Tab. 2 indicates that the accuracies of all approaches employing GASF surpass those utilizing the Hilbert transform. The RepVGG-A0 + GASF technique exhibits the highest accuracy, the accuracy of ResNet18 + GASF, although comparable to RepVGG-A0 + GASF, is notably inferior for model inference time and size. Fig. 4 illustrates the accuracy variation curves for the training and validation sets of the experiment.

Fig. 4 illustrates that RepVGG-A0 + GASF exhibits a more rapid convergence compared to the other three approaches. All four strategies can attain approximately 100% accuracy in the training set. The validation set exhibits significant fluctuations following the convergence of ResNet18 + GASF, accompanied by a little overfitting phenomena. In comparison to the other

three approaches, RepVGG-A0 + GASF exhibits faster convergence, more stability post-convergence, superior accuracy, and a reduced tendency for overfitting.

Fig. 5 illustrates that the network using RepVGG-A0 combined with the Hilbert method easily confuses target H and target B. A similar confusion between target H and target B can also be observed in the ResNet18 combined with the Hilbert method. However, when using GASF, neither method exhibits confusion between these two targets, and each target maintains a relatively high accuracy. This demonstrates that the GASF method can better distinguish the features of IQ signals compared to the Hilbert method.

5 Conclusion

This paper proposes a method for specific emitter identification based on RepVGG and GASF. The method integrates RepVGG and GASF to extract IQ signal properties in three dimensions: In-phase, Quadrature, and Modul. The intricate characteristics of IQ signals are integrated to derive state vectors. In comparison to the ResNet18 network and the Hilbert transform approach, the experimental findings indicate that the suggested method exhibits superior accuracy, reduced training time, and a smaller model size, rendering it more appropriate for deployment on hardware platforms.

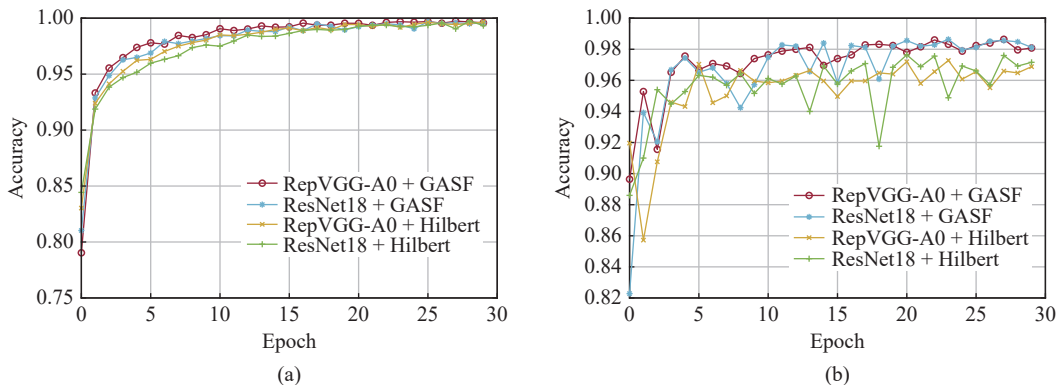


Fig. 4 Accuracy variation curve: (a) training set; (b) validation set

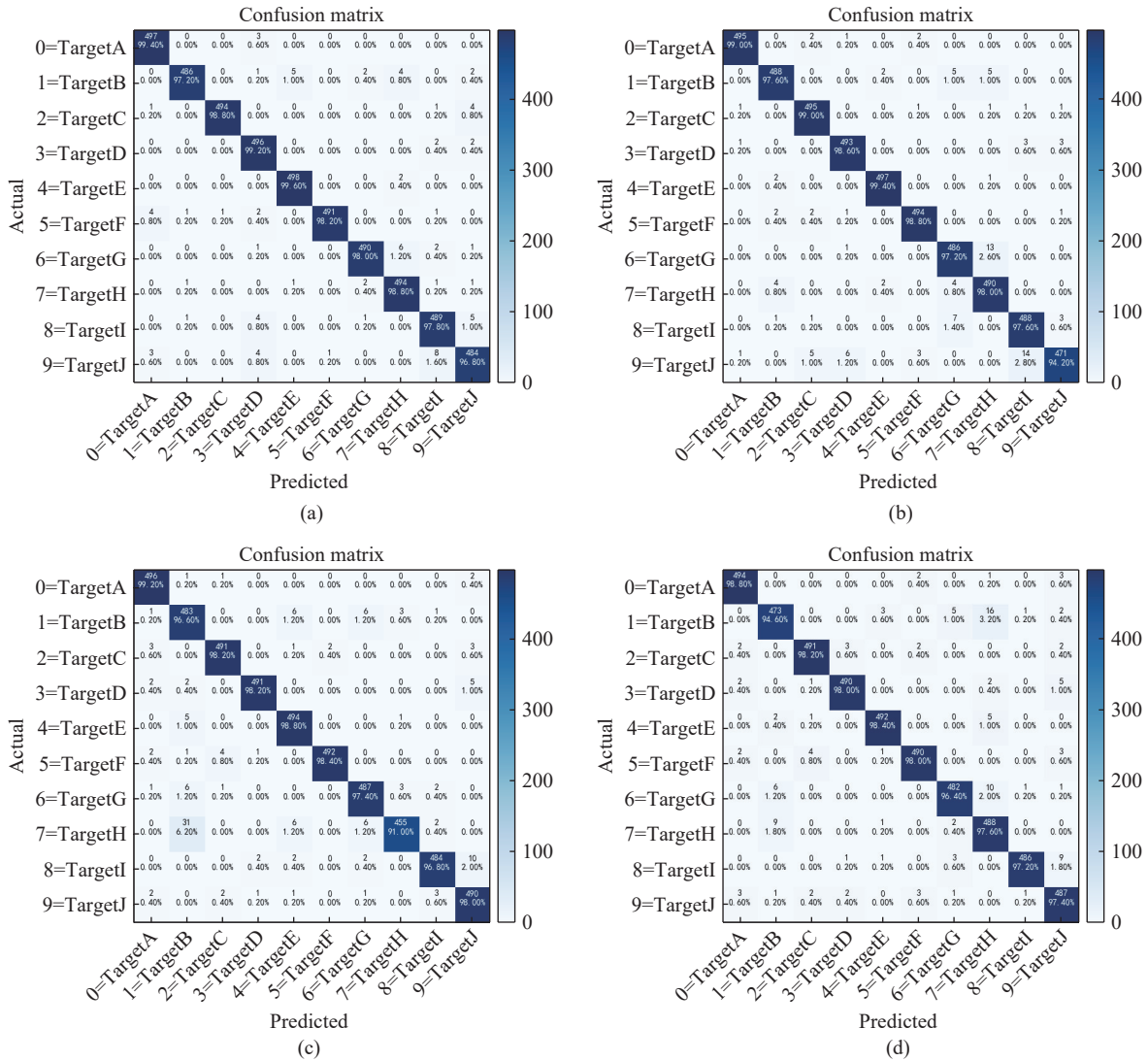


Fig. 5 Classification confusion matrix: (a) RepVGG-A0 + GASF; (b) ResNet18 + GASF; (c) RepVGG-A0 + Hilbert; (d) ResNet18 + Hilbert

References:

- [1] Y. K. Gok, Y. K. Alp and O. Arikan, "A new method for specific emitter identification with results on real radar measurements," *IEEE Transactions on Information Forensics and Security*, vol. 15, pp. 3335-3346, 2020.
- [2] Y. Zheng, J. Wang, and J. Huang, "Open space radar specific emitter identification using MSAK-CNN-LSTM network," *IET Radar, Sonar & Navigation*, vol. 18, pp. 1080-1093, 2024.
- [3] G. Zhang, "Research on radar radiation source identification technology," Ph. D. dissertation, National University of Defense Technology, 2023.
- [4] Y. Xu, S. Cheng S, X. Dong X, Y. Z. Hou, and P. Donget, "Radar radiation source individual recognition based on DBN feature extraction," *Journal of Air Force Engineering University: Natural Science Edition*, vol. 20, no. 6, pp. 7, 2019.
- [5] P. Leng and Z. Xu, "A deep reinforcement learning method for radar radiation source individual recognition," *Acta Ordnance Engineering*, vol. 39, no. 12, pp. 7, 2018.
- [6] H. Wang, G. Zhao, and Y. Wang, "Radiation source individual recognition based on high-order moment characteristics of pulse envelope front," *Modern Radar*, no. 10, pp. 5, 2010.
- [7] Y. Xiao and X. Z. Wei, "Specific emitter identification of radar based on one dimensional convolution neural network," *Journal of Physics Conference Series*, vol. 1550, pp. 032114, 2020.
- [8] B. Wu, S. Yuan, P. Li, Z. Jing, S. Huang, and Y.

Zhao, "Radar emitter signal recognition based on one-dimensional convolutional neural network with attention mechanism," *Sensors*, vol. 20, pp. 6350, 2020.

- [9] S. D. Wickramaratne and S. Mahmud, "A deep learning based ternary task classification system using gramian angular summation field in fNIRS neuroimaging data," in *International Conference on E-Health Networking, Applications and Services*, Shenzhen, China, pp. 1-4, 2020.
- [10] X. Ding, X. Zhang, N. Ma, J. Han, G. Ding, and J. Sun, "RepVGG: Making VGG-style ConvNets great again," in *IEEE/CVF Conference on Computer Vision and Pattern Recognition (CVPR)*, Nashville, TN, USA, pp. 13728-13737, 2021.
- [11] A. J. Yin, M. Y. Lv, M. Y. Yang, and X. M. Chen, "Bearing fault diagnosis based on the combined use of RepVGG and CapsNet," *Journal of Vibration and Shock*, vol. 43, no. 14, pp. 301-307, 2024.



Dequo Zeng received the B.E., and Ph.D. degrees in signal processing from University of Electronic Science and Technology of China, Chengdu, China, in 2007, and 2012. His research interests include electronic countermeasures and signal recognition.



Fuyuan Xu received the B.E., and Ph.D. degrees in electrical engineering from the Nanjing University of Science and Technology, Nanjing, China, in 2009, and 2016. His research interests include target tracking and machine learning.



Jin Qin is an experienced researcher in the field of the electronic countermeasures. His research interests include signal identification and artificial intelligence.



Zhenyi Yao is the master at the Nanjing University of Aeronautics and Astronautics. His current research interests focus on signal identification and flight control systems.



Zuyue Shang received the master degree of computer technology in University of Chinese Academy of Sciences, Chengdu, China, in 2020. His research interests include electronic countermeasures and machine learning.